PII: S0032-3861(97)00064-5

Polymer Vol. 38 No. 21, pp. 5411–5418, 1997

0032-3861/97/$17.00 + 0.00

Crystallization behaviour of fractions of a copolymer of propene and 1-hexane

Ernesto Pérez*, Rosario Benavente, Antonio Bello and José M. Pereña
Instituto de Ciencia y Tecnología de Polímeros del CSIC, Juan de la Cierva 3, 28006-Madrid, Spain

and Debora Zucchi and Maria Carmela Sacchi
Instituto di Chimica delle Macromolecole del CNR, Via E. Bassini 15, 20133-Milano, Italy
(Revised 10 December 1996)

The crystallization behaviour of seven fractions of a copolymer of propene and 1-hexane has been analysed. The fractionation discriminates simultaneously in comonomer content, stereoregularity and molecular weight, in such a way that the fraction obtained first at the lowest temperature displays the lowest molecular weight and isotactic triads fraction and the highest comonomer content. The crystallization rate of this fraction is very slow and it does not crystallize in the calorimeter when cooled from the melt at usual rates. The variation of different thermal parameters with the composition of these fractions has been analysed, as well as the crystallinity, determined by differential scanning calorimetry, X-ray diffraction and density measurements. Isothermal experiments enable us to obtain the extrapolated melting temperatures of these fractions and the Avrami exponent for the crystallization, which has been found to be close to three in all the cases. Non-isothermal experiments have also been analysed, comparing the results with the isothermal ones.

(Keywords: propene-1-hexane copolymer fractions; crystallization behaviour; degree of crystallinity)

INTRODUCTION

Random copolymers of polypropene are important commercial products, with applications such as films requiring good clarity, flexibility and mechanical strength[1]. At present, these copolymers can be obtained both from heterogeneous and homogeneous catalysts.

A satisfactory knowledge of the structure–properties relationships of any polymer requires, among other factors, analysis of the crystallization behaviour. Unfortunately, many variables are present when studying propene copolymers, for example comonomer compositions, stereoregularity, heterogeneity and molecular weight are of capital importance. In addition, isotactic polypropene (iPP) displays a polymorphic behaviour[2–6] and the presence of defects, like comonomer units, is supposed to favour the formation of the γ modification.

In a previous paper[7] we have analysed the thermal and viscoelastic behaviour of some of these copolymers as a function of composition. They were synthesized by a Ziegler–Natta catalyst containing electron-donor substances in order to increase the stereoregularity of the products. It is well known that these catalysts lead to heterogeneous polymers[8,9].

The aim of this paper is to analyse the crystallization behaviour of the fractions obtained from one of those copolymers. This work is part of a more general study of the properties of propene copolymers synthesized with different catalyst systems, both homogeneous and heterogeneous.

*To whom correspondence should be addressed

EXPERIMENTAL

Seven fractions, obtained by extracting a propene-1-hexene copolymer with octane at different temperatures (20, 45, 65, 80, 90, 100 and 110°C, respectively), have been studied. The details of the copolymer fractionation have been reported elsewhere[10]. The copolymer, named PHF24, was obtained with the catalyst $MgCl_2$/diisobutylphthalate/$TiCl_4$, with triethoxyphenylsilane as external donor. The molar fraction of isotactic triads, [mm], and comonomer content (mol%) are shown in *Table 1* for the seven fractions and the unfractionated copolymer.

Molecular weights were determined by size exclusion chromatography (s.e.c.) in Waters 150C equipment, in trichlorobenzene at 145°C. Twelve samples of monodisperse polystyrene (with molecular weights ranging from 1800 to 2 300 000) were used as standards, considering the M_{peak} representative of the whole of the sample. A differential refractive index detector and a differential viscometer Viscotek 110, working at 145°C, were coupled at the end of the columns. The molecular weight results are shown in the last two columns of *Table 1*. It can be observed in this table that the fractionation discriminates simultaneously in comonomer content, stereoregularity and molecular weight.

Calorimetric analyses were carried out in a Perkin-Elmer DSC7 calorimeter, connected to a cooling system and calibrated with different standards. About 7 mg of sample were used. The heat of fusion of a perfect polypropene crystal, used in the determination of the crystallinity, was taken[11] as 209 J g^{-1}.

Isothermal methods were used for the analysis of the

Table 1 Weight fraction, comonomer content (mol%), molar fraction of isotactic triads [mm] and molecular weights of the samples

Sample	Fraction (wt%)	Hexene content (mol%)	[mm]	M_n	M_w/M_n
PHF247	26.26	1.03	0.984	71 700	2.55
PHF246	11.46	1.47	0.977	–	–
PHF245	11.46	2.53	0.972	29 800	2.52
PHF244	9.24	3.40	0.924	–	–
PHF243	7.81	4.59	0.904	26 900	3.02
PHF242	3.22	6.60	0.852	–	–
PHF241	30.49	9.48	0.635	9900	2.22
PHF24	–	4.70	0.880	35 500	3.23

crystallization kinetics: the samples were brought from the melt to the desired crystallization temperature, T_c, and the heat evolution was registered as a function of time. The melting temperatures of these isothermally crystallized samples were determined by heating from the corresponding T_c at 5°C min^{-1} after the crystallization was complete. Non-isothermal methods were also employed, recording the crystallization from the melt at different cooling rates, ranging from 3 to 40°C min^{-1}.

Wide-angle X-ray diffractograms (WAXD) were recorded at room temperature by using a Philips diffractometer with a Geiger counter, connected to a computer. Ni-filtered Cu–K_α radiation was used. The diffraction scans were collected over a period of 15 min between 2θ values of 5° and 35° using a sampling rate of 1 Hz. The films for WAXD were prepared by cooling from the melt under a little pressure. Not all the fractions were analysed, due to the reduced amount of sample.

Specimen densities were measured at 20°C using a density gradient column filled with an ethanol–water mixture. The crystallinity was calculated assuming a two-phase model and values of $\rho_a = 0.852$ g cm^{-3} and $\rho_c = 0.936$ g cm^{-3} for the amorphous and crystalline densities, respectively[12].

RESULTS AND DISCUSSION

Thermal behaviour

The differential scanning calorimetry (d.s.c.) cooling traces, obtained at 20°C min^{-1}, of the seven fractions are shown in the upper part of *Figure 1*. A steady decrease of the minimum of the crystallization exotherm can be observed as the comonomer content of the fraction increases (or the value of [mm] decreases). Moreover, the exotherms widen appreciably (and the enthalpy gets smaller), indicating an increasing difficulty of the crystallization, in such a way that fraction PHF241 is not able to crystallize at that cooling rate. The subsequent melting of these samples is shown in the lower part of *Figure 1*. Several aspects can be observed in this figure. First, the melting temperatures and the heat of melting decrease from PHF247 to PHF241. Second, a clear cold crystallization can be observed for PHF241, since this fraction was not able to crystallize on cooling at 20°C min^{-1}. Third, the increase of heat capacity characteristic of the glass transition is now very evident for the fractions with higher comonomer content, owing to their lower crystallinities (sample PHF241 is supposed to be totally amorphous when cooled to 20°C min^{-1} below the glass transition temperature, T_g). The final aspect from *Figure 1* is that the d.s.c. melting curves show two endothermic peaks partially overlapped, less defined for the fractions with higher comonomer content.

The nature of these two peaks was investigated by performing melting experiments at different rates after the same crystallization conditions. For instance, *Figure 2* shows the melting curves at 10 and 20°C min^{-1} after crystallization by cooling at 20°C min^{-1} in both cases. The fact that the relative proportion of the two peaks changes with the heating rate, with a smaller high-temperature component at the higher rate, points in favour of the second peak being due to a recrystallization of the first one. Evidently, this recrystallization will be

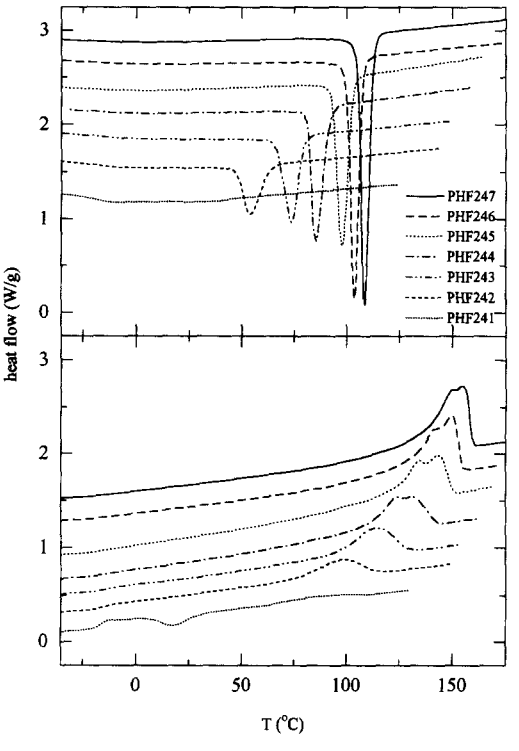

Figure 1 D.s.c. cooling curves, at 20°C min^{-1} (upper) and subsequent heating runs, at 10°C min^{-1} (lower) for the different fractions

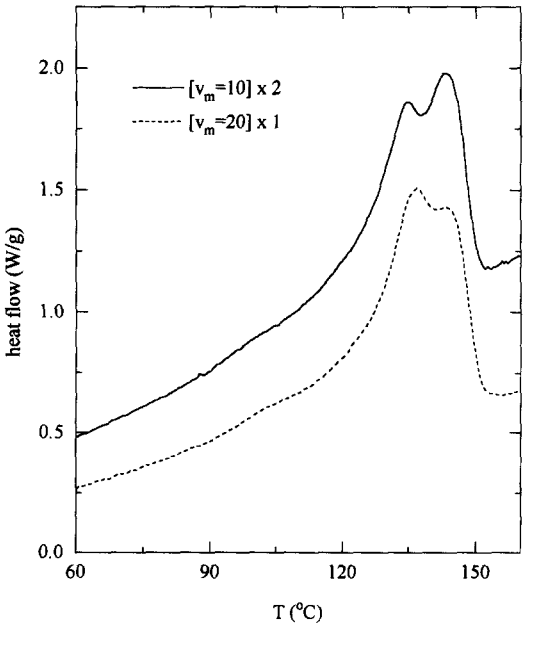

Figure 2 Effect of the heating rate, v_m, on the melting curve of fraction PHF245 crystallized from the melt at 20°C min^{-1}. The curve with $v_m = 10$°C min^{-1} has been multiplied by 2 for a better visualization

possible if the length of the initial crystals is smaller than the total length of crystallizable segments. In the case of high comonomer contents or low stereoregularity, the length of crystallizable segments will be rather small and the recrystallization ability is expected to diminish, considering that stereo errors and comonomer units cannot be included in the crystal lattice. This is consistent with the fact that the higher temperature component of the endotherms in *Figure 1* diminishes as the comonomer content increases. Further evidence of this recrystallization phenomenon will be found later in the isothermal experiments.

The d.s.c. results for the different fractions are summarized in *Table 2*, where T_m represents the temperature of the low temperature component of the endotherms, supposed to be the real melting before recrystallization. The values of T_g, T_m and enthalpy of melting, ΔH_m, have been plotted in *Figure 3* as a function of the comonomer content. The observed behaviour is consistent with a decrease in size and perfection of the crystallites and an increase in the amount of the amorphous phase. Evidently, the decreasing of these magnitudes is due to both the increase in comonomer content and the decrease of the [mm] content (a much smaller effect of molecular weight is also expected). Some idea of the independent effect of those two variables can be extracted from the data of ΔH_m for the unfractionated copolymers in ref. 7, plotted as solid symbols in the upper part of *Figure 3*. These copolymers (and the homopolymer) all have the same [mm] content, 0.88, and they have been synthesized with the same catalyst system. It can be observed that the decrease of ΔH_m in relation to the homopolymer for these unfractionated samples is approximately one half of that one for the fractions of the present work (we plan to analyse different copolymer fractions in order to investigate more adequately the independent effect of those two variables).

Table 2 Glass transitions, T_g (extrapolated at zero heating rate), actual melting temperatures, T_m, enthalpies of melting, ΔH_m, melting temperatures, T_m^* (extrapolated by the $T_m - T_c$ method) and slopes of the corresponding representations, for the different samples

Sample	T_g (°C)	T_m (°C)	ΔH_m (J g^{-1})	T_m^* (°C)	Slope
PHF247	−10	149	88	174	0.48
PHF246	−10	142	80	171	0.48
PHF245	−12	134	78	162	0.46
PHF244	−12	123	69	153	0.47
PHF243	−13	114	55	142	0.47
PHF242	−14	98	42	–	–
PHF241	−15	88	12	–	–
PHF24	−11	142	62	–	–

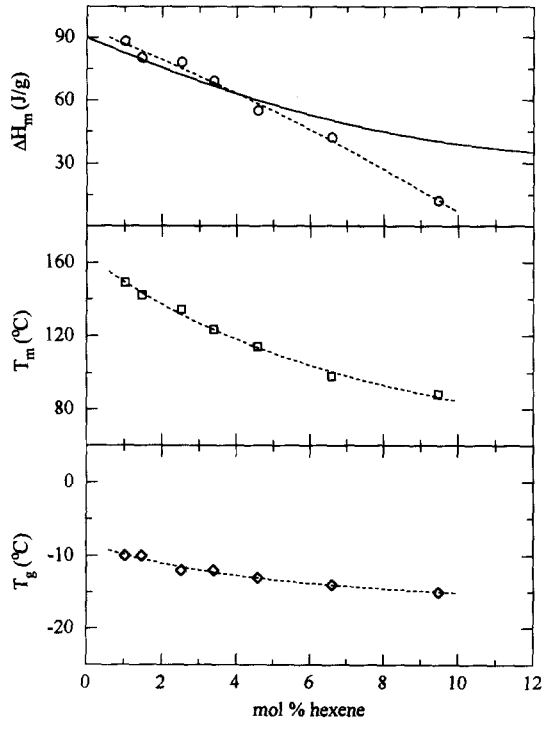

Figure 3 Variation of the enthalpy of melting, melting temperature and glass transition temperature with the composition of the fractions, crystallized from the melt at 20°C min^{-1}. The continuous line in the upper part, taken from ref. 7, corresponds to unfractionated copolymers with a [mm] content of 0.88

Isothermal experiments

The fractions were isothermally crystallized in different temperature intervals, depending on their crystallization temperatures. The intervals range from the lowest temperature where the crystallization begins just after baseline equilibration to the highest temperature where the noise level still allows reliable calculations on the isotherm. However, the isotherms present a considerable level of noise at any crystallization temperature for the two fractions with higher comonomer content, PHF242 and PHF241, due mainly to their reduced crystallinity attainable.

For the remaining five fractions, the melting endotherms were also recorded after isothermal crystallization. A heating rate of 5°C min^{-1} was chosen in order to minimize the interval for temperature equilibration and still have a good signal-to-noise ratio. This relatively low heating rate is expected to emphasize possible recrystallization phenomena. A selection of these melting endotherms for three of the fractions is presented in *Figure 4*. All the samples exhibit multiple endotherms. The upper temperature peak becomes less marked with increasing crystallization temperature and its position does not change appreciably with T_c, as expected for a recrystallization phenomenon. Moreover, the recrystallization process is less marked as the comonomer content increases. Establishing the nature of the endotherms is important in the analysis of the equilibrium melting temperature by the $T_m - T_c$ extrapolation method. Our experience with other iPP samples is that important errors can be derived from this extrapolation, since from higher heating rates and samples of high isotactic content the recrystallization peak cannot be clearly resolved from the real melting peak. In the present case, since the double melting behaviour is attributed to a melting and recrystallization process during fusion, the low temperature endotherm is therefore used for the extrapolation, since it is assumed to arise from the crystals formed at T_c, before recrystallization. Those extrapolations are shown in *Figure 5* for the five fractions where the isothermal crystallization has been analysed. The values for the extrapolated melting temperatures, T_m^*, to the line $T_m = T_c$ and the slopes of the corresponding straight lines are shown in *Table 2*. The slopes are in all the cases practically equal to the theoretical value of 0.5. Moreover, a clear decrease of the extrapolated melting temperature is observed.

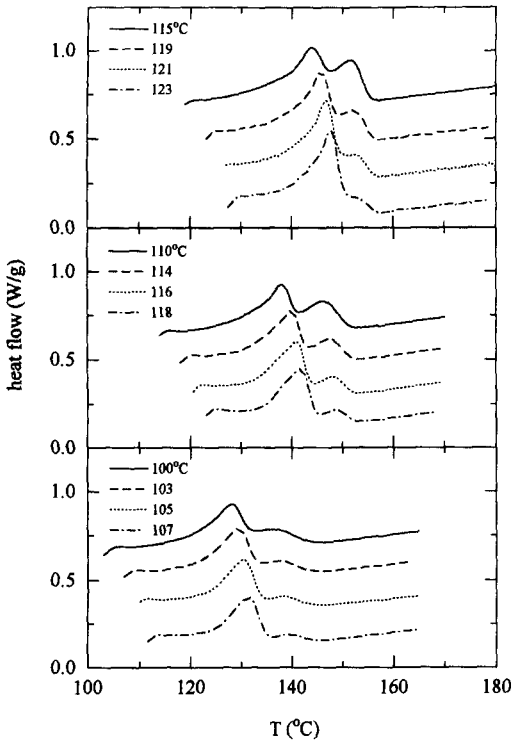

Figure 4 Selected melting curves, at 5°C min^{-1}, corresponding to fractions PHF246 (upper), PHF245 (middle) and PHF244 (lower) after isothermal crystallization at the indicated temperatures

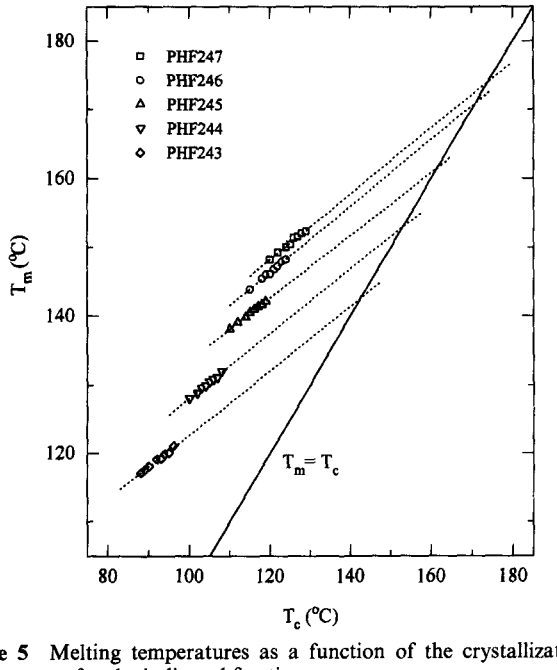

Figure 5 Melting temperatures as a function of the crystallization temperatures for the indicated fractions

It was mentioned above that the presence of comonomer units and stereo errors are supposed to favour the formation of the γ phase, as well as crystallization at high temperatures[5]. Although we have found only the α form in films of these samples (see below), the formation of the γ phase cannot be disregarded, especially at high values of T_c and for those fractions with higher comonomer content (and lower stereoregularity). Anyway, there is no appreciable discontinuity or change of the slope in the representation of *Figure 5*. These results lead us to conclude that there is no significant amount of γ phase under the present crystallization conditions or the melting points of the two forms are the same.

These fractions have simultaneously different comonomer content, [mm] fraction and molecular weight, and therefore a multidimensional plot would be necessary to display the variation of the melting temperature (or any other magnitude). The corresponding extrapolation to comonomer content = 0, [mm] = 1 and infinite molecular weight will represent the equilibrium melting temperature, T_m^0, of pure iPP. *Figure 6* shows the variation of T_m^* with the hexene content of the fractions, i.e. it represents one of the projections of the mentioned multidimensional plot. A rather smooth and linear dependence is observed, and the extrapolation to zero comonomer content gives the value of 184°C, in good agreement with most other estimations of T_m^0 for iPP[13–15].

To get an idea of the independent effect of the different variables on the value of T_m^*, we have used different approximations. The effect of molecular weight can be estimated from the following equation[16]:

$$T_m = 460.8(x - 4.893)/(x + 0.807 \ln x - 3.109) \quad (1)$$

where x is the degree of polymerization (a value of $T_m^0 = 460.8$ K, i.e. 187.6°C, is implied). With this equation, a depression of the melting temperature of the order of 5°C is obtained for fraction PHF243, which is the one with lowest molecular weight of those where we have the value of T_m^*.

The effect of comonomer units can be also estimated by using the formulations of Sanchez and Eby[17] and Helfand and Lauritzen[18] for random copolymers. By assuming that the 1-hexene units are excluded from the iPP lattice, those theories reduce to the Flory equation[19] for the exclusion model:

$$\frac{1}{T_m^0} - \frac{1}{T_m} = \frac{R}{\Delta H_u} \ln(1 - X) \quad (2)$$

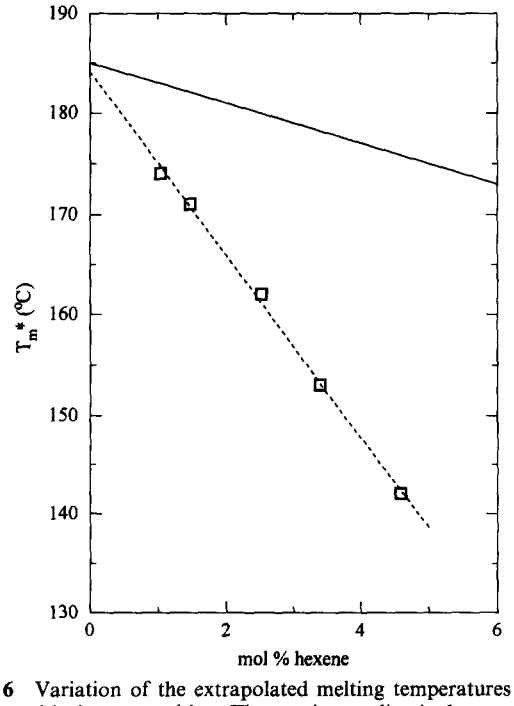

Figure 6 Variation of the extrapolated melting temperatures of the fractions with the composition. The continuous line is the representation of equation (2) (see text)

where X is the mole fraction on non-crystallizable units. This equation has been plotted in *Figure 6* (continuous line) using[20] $T_m^0 = 185°C$ and $\Delta H_u = 8.7\,kJ\,mol^{-1}$. From this equation, a depression of 10°C is predicted for fraction PHF243 due to the presence of 1-hexene units randomly distributed.

Adding the two contributions of molecular weight and comonomer units, a depression of 15°C is obtained, while the experimentally observed depression is of the order of 42°C. It seems, therefore, that the major contribution to the melting point depression is due to the presence of stereoirregular units. This contribution might be also estimated from the mentioned theories[17,18], provided that the model of crystallization is known. A uniform exclusion model seems to fit the experimental data of iPP with different isotactic contents[20].

The crystallization isotherms of our fractions have been analysed in terms of the Avrami equation[21]:

$$X_c(t) = 1 - \exp(kt^n) \quad (3)$$

where k is a kinetic constant of the crystallization process and the exponent n is a parameter defining the mode of nucleation and crystal growth geometry. The extent of the transformation at time t, $X_c(t)$, is determined from the isothermal curves as the ratio of the enthalpy evolved at time t to that of the overall process.

The Avrami equation is usually represented as a double logarithmic plot, as in *Figure 7* for sample PHF244. It can be observed that this equation is followed up to relatively high conversions. The values of n and k, illustrated in *Tables 3* and *4*, were obtained by linear least-squares fits of the data in the initial linear portions of each isotherm. Regarding the values of n, it seems that there is a tendency for a decrease of this exponent when the undercooling, ΔT, decreases for a given sample. When comparing the different fractions, it seems also that the Avrami exponent decreases slightly when the comonomer content increases. Anyway, the

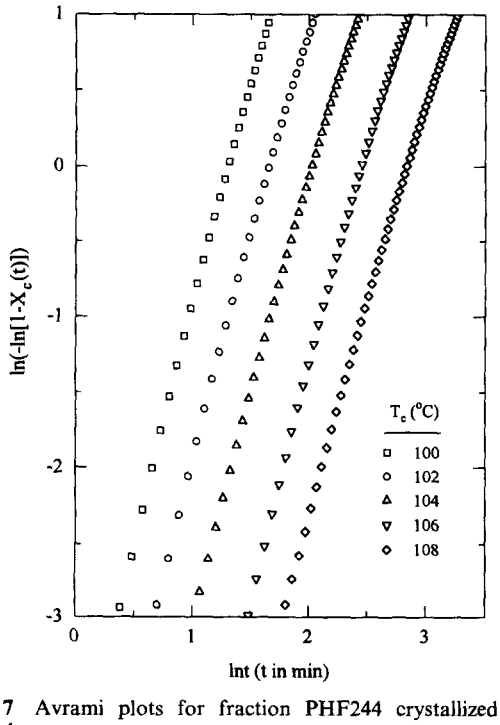

Figure 7 Avrami plots for fraction PHF244 crystallized at the indicated temperatures

Table 3 Avrami exponent for the isothermal crystallization of the fractions

	Avrami exponent, n				
ΔT^a	PHF247	PHF246	PHF245	PHF244	PHF243
56	–	3.6	–	–	–
54	3.5	–	–	–	3.1
53	–	3.3	–	3.0	3.0
52	3.4	3.3	3.4	–	2.8
51	–	3.1	–	2.9	–
50	3.4	3.1	3.2	2.8	2.8
49	3.2	3.1	–	2.8	2.8
48	3.1	2.9	3.3	2.7	2.8
47	3.1	–	2.9	2.8	2.5
46	2.9	–	2.9	2.7	2.5
45	2.8	–	2.8	2.7	–
44	–	–	2.8	–	–
n_{av}	3.2 ± 0.2	3.2 ± 0.2	3.0 ± 0.2	2.8 ± 0.1	2.8 ± 0.2

$^a\Delta T = T_m^* - T_c$

Table 4 Kinetic constants for the isothermal crystallization of the fractions

	Kinetic constant, k (min^{-n})				
ΔT^a	PHF247	PHF246	PHF245	PHF244	PHF243
56	–	1.13×10^{-2}	–	–	–
54	1.74×10^{-2}	–	–	–	1.20×10^{-2}
53	–	1.42×10^{-3}	–	1.89×10^{-2}	9.28×10^{-3}
52	3.74×10^{-3}	6.69×10^{-4}	1.72×10^{-2}	–	6.60×10^{-3}
51	–	4.76×10^{-4}	–	8.40×10^{-3}	–
50	6.36×10^{-4}	2.23×10^{-4}	4.52×10^{-3}	6.28×10^{-3}	2.58×10^{-3}
49	3.67×10^{-4}	1.20×10^{-4}	–	3.38×10^{-3}	1.99×10^{-3}
48	2.66×10^{-4}	1.12×10^{-4}	8.17×10^{-4}	2.55×10^{-3}	1.21×10^{-3}
47	1.12×10^{-4}	–	7.39×10^{-4}	8.67×10^{-4}	1.40×10^{-3}
46	9.42×10^{-5}	–	5.00×10^{-4}	8.94×10^{-4}	1.10×10^{-3}
45	5.44×10^{-5}	–	3.22×10^{-4}	5.11×10^{-4}	–
44	–	–	2.10×10^{-4}	–	–

$^a\Delta T = T_m^* - T_c$

average values of n, reported also in *Table 3*, are very close to 3 in all the cases. The interpretation of this value of n is that the primary nucleation of these samples seems to be heterogeneous followed by a three-dimensional growth.

Regarding the values of k (see *Table 4*), it seems that, for the same undercooling, they increase, in general, with the number of defects in the fraction. Deviations from this general trend may be due, first, to uncertainties in the total time for the crystallization to be completed, the second, to errors in the estimation of the value of T_m^* and, therefore, in the undercooling. In fact, it may be deduced from *Table 4* that a much more smooth variation of k will be obtained if the value of T_m^* were 2° lower for PHF246 and 2° higher for PHF245 (evidently, the extrapolations in *Figure 5* to obtain T_m^* involve an error of at least 2°). In such case, all the values in *Table 4* will begin and end at almost the same values for the undercooling, considering, moreover, that the actual crystallization interval is 8°C for all the fractions (except for PHF247, which is 9°C).

However, the changes with the undercooling of the overall rate constant, k, are different for the five fractions: from *Table 4* it is deduced that in 8° the increase in k ranges from more than two orders of magnitude for PHF247 to only about one order for PHF243. It is evident that the increase of the atactic and comonomer content have a large effect on the overall rate of crystallization.

Wide angle X-ray diffraction

Figure 8 shows the WAXD profiles of three of the fractions (PHF247, PHF246 and PHF241) together with the unfractionated copolymer PHF24. All these samples display the well-known WAXD usually observed for the monoclinic α phase, although it is postulated that the γ phase is favoured by the presence of errors like comonomer units or stereo errors[22]. Unfortunately, the limited amount of sample for these fractions did not allow us to perform a detailed analysis of the influence of the crystallization conditions on the possible formation of γ phase.

A broadening of the characteristic X-ray peaks with increasing comonomer content can be observed in *Figure 8*, resulting from a decrease in size and perfection of crystallites. A rough deconvolution of the diffractogram between amorphous and crystalline components allowed to estimate the crystallinities. *Figure 9* shows the comparison of the crystallinities estimated from the enthalpy of melting with those ones determined from X-ray diffraction and from density measurements, for the fractions where the quantity of sample was enough for these determinations. As usual in polyolefins, the density estimations for the crystallinity fraction are somewhat higher than those from d.s.c. (about 0.17–0.22 higher in the present case), the difference being due to the interfacial content, which does not contribute to the enthalpy of melting[23,24].

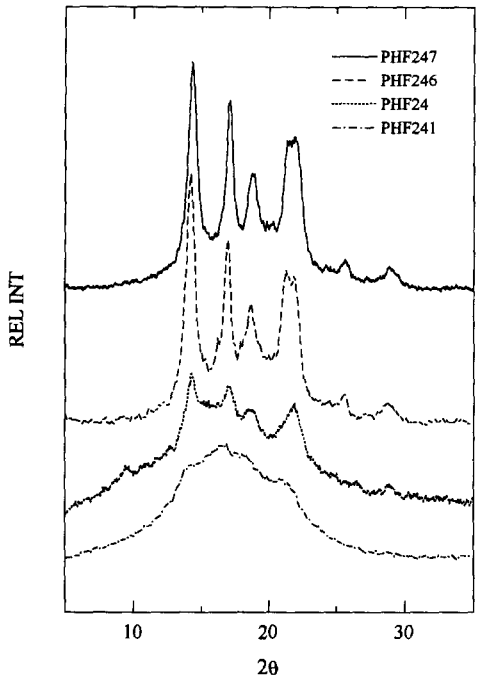

Figure 8 X-ray diffractograms for the unfractionated sample (PHF24) and three of the fractions

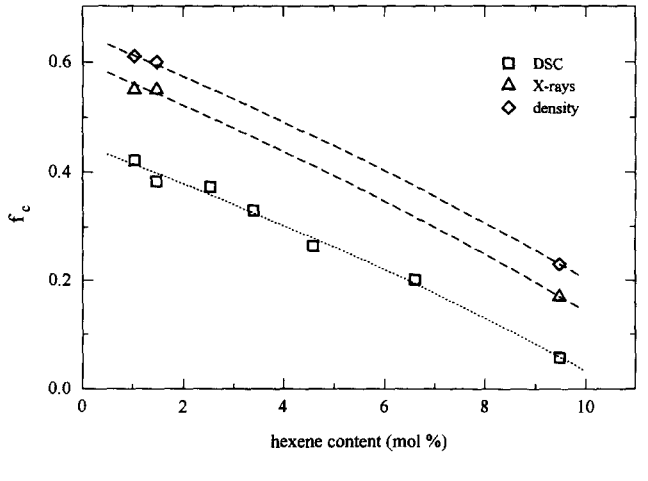

Figure 9 Variation of the crystallinity, determined by d.s.c., X-rays and density, as a function of the composition for the different fractions

Non-isothermal crystallization

The study of non-isothermal crystallization kinetics can be a very good alternative to isothermal kinetics in some cases. The majority of the formulations proposed for non-isothermal studies are based on Avrami-type equations. One of the more usual theories is that of Ozawa[25], where it is assumed that when a polymer is

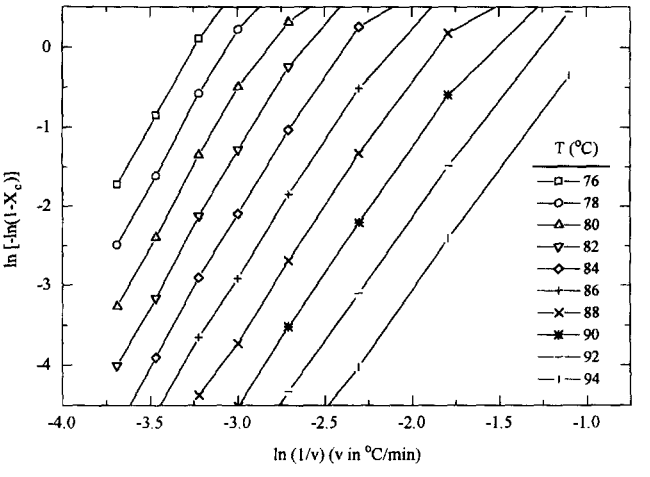

Figure 10 Representation of the Ozawa equation for fraction PHF244

Table 5 Avrami exponent for the non-isothermal crystallization of the fractions

	n					
ΔT^a	PHF247	PHF246	PHF245	PHF244	PHF243	PHF242[b]
80	–	–	–	–	–	2.5
78	–	–	–	–	3.3	–
77	–	–	–	3.6	–	–
76	–	–	–	–	3.4	2.4
75	–	4.2	–	3.6	–	–
74	–	–	3.9	–	3.5	–
73	–	4.3	–	3.4	–	–
72	4.2	–	3.8	–	3.3	2.3
71	–	4.5	–	3.5	–	–
70	4.4	–	3.8	–	3.5	–
69	–	4.5	–	3.3	–	–
68	4.6	–	4.1	–	3.5	2.2
67	–	4.2	–	3.2	–	–
66	4.3	–	3.8	–	3.2	–
65	–	4.0	–	3.0	–	–
64	3.9	–	3.6	–	3.0	2.0
63	–	3.8	–	2.9	–	–
62	3.6	–	3.5	–	2.9	–
61	–	3.6	–	2.8	–	–
60	3.4	–	3.1	–	–	1.9
59	–	3.3	–	2.6	–	–
58	3.3	–	3.3	–	–	–
56	–	–	–	–	–	1.8
n_{av}	4.0 ± 0.5	4.0 ± 0.4	3.7 ± 0.3	3.2 ± 0.4	3.3 ± 0.2	2.2 ± 0.3

[a] $\Delta T = T_m^* - T_c$

[b] Considering a value of $T_m^* = 124°C$, extrapolated from *Figure 6*

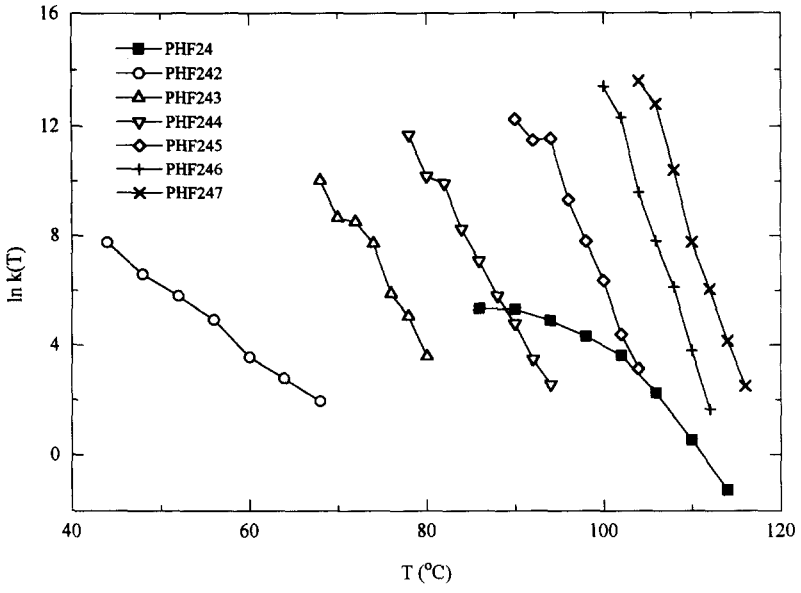

Figure 11 Variation of $\ln k(T)$ with temperature for the unfractionated copolymer (PHF24) and several fractions

cooled from the melt at a certain rate the crystallization at a given temperature proceeds from a distribution of nuclei growing at a constant rate. With this assumption, the Ozawa equation reads:[25]

$$-\ln(1 - X_c) = \frac{k(T)}{v^n} \tag{4}$$

where X_c is the degree of transformation at a temperature T, v is the cooling rate, n is again the Avrami exponent and $k(T)$ is a cooling crystallization function, which depends exponentially on T and includes the free energy term of the process[25]. (The Ozawa equation can also be used in the non-isothermal crystallization from the quenched state, and then v is the heating rate and $k(T)$ a heating function.)

The Ozawa theory has been applied to the present samples in the range of cooling rates from 3 to 40° min^{-1}. The exception is fraction PHF241, whose crystallinity is very small, as mentioned before, and can only crystallize from the melt at very low cooling rates. For the remaining fractions, the corresponding data of degree of transformation at a given temperature and cooling rate can be analysed according to the Ozawa equation, which can be rearranged as follows:

$$\ln[-\ln(1 - X_c)] = \ln k(T) + n \ln\left(\frac{1}{v}\right) \tag{5}$$

Fairly good straight lines are obtained for the present samples. For instance, the representation of this equation for fraction PHF244 can be seen in *Figure 10*. The conclusion is, then, that the non-isothermal crystallization of these samples can be analysed in terms of the Avrami equation.

The Avrami exponent and the cooling function have been obtained, respectively, from the slope and intercept of these straight lines, after correction of the thermal lag between the temperature of the sample and the holder[26]. The corresponding values of n are listed in *Table 5*. Comparing with *Table 4*, it can be observed that the non-isothermal temperature range is just below the isothermal one, and the higher values of n are obtained in the non-isothermal case. Moreover, it seems to be confirmed that the Avrami exponent increases with the undercooling and decreases when the comonomer content increases. In this regard, it may be important to note that the unfractionated sample, PHF24, has been also non-isothermally crystallized. The results show values of n in the range 1.6–2.0, in the temperature interval from 86 to 114°C. It seems, therefore, that abnormally low values of the Avrami exponent are obtained in non-fractionated samples, probably due to the selective crystallization of chains with less defects at the higher temperatures. (The values of n reported from the use of the Ozawa equation for a commercial iPP sample[26] are of the order of 3.)

Abnormal behaviour is also shown by the unfractionated copolymer in the values of the cooling function, as shown in *Figure 11*. While the logarithmic representation of the cooling function is almost linear for the fractions, a very different behaviour is shown by the unfractionated sample.

In conclusion, the kinetic parameters of these copolymers are greatly influenced by polydispersity, and the results obtained from unfractionated samples have to be handled with caution.

ACKNOWLEDGEMENTS

The financial support of the EEC (Network ERBCHRXCT930158) and of the Comisión Interministerial de Ciencia y Technología (project no. PB94-1529) is gratefully acknowledged. We are also indebted to Dr M. Aroca, of Repsol Química S.A., for the molecular weight determinations.

REFERENCES

1. Galli, P., *Prog. Polym. Sci.*, 1994, **19**, 959.
2. Turner-Jones, A., Aizlewood, J. M. and Beckett, D. R., *Makromol. Chem.*, 1964, **75**, 134.
3. Meille, S. V., Ferro, D. R. and Brückner, S., *Macromol. Symp.*, 1995, **89**, 499.
4. Fischer, D. and Mülhaupt, R., *Macromol. Chem. Phys.*, 1994, **195**, 1433.
5. Alamo, R. G., Lucas, J. C. and Mandelkern, L., *Polymer Prepr.*, 1994, **35**, 406.

6. O'Kane, W. J., Young, R. J., Ryan, A. J., Bras, W., Derbyshire, G. E. and Mant, G. R., *Polymer*, 1994, **35**, 1352.
7. Benavente, R., Pereña, J. M., Bello, A., Pérez, E., Locatelli, P., Fan, Z.-Q. and Zucchi, D., *Polymer Bull.*, 1996, **36**, 249.
8. Mirabella, F. M. and Ford, E. A., *J. Polymer. Sci., B, Polym. Phys.*, 1987, **25**, 777.
9. Hosoda, S., *Polymer J*, 1988, **20**, 283.
10. Fan, Z.-Q., Forini, F., Tritto, I., Locatelli, P. and Sacchi, M. C., *Macromol. Chem. Phys.*, 1994, **195**, 3889.
11. Clark, E. J. and Hoffman, J. D., *Macromolecules*, 1984, **17**, 878.
12. Brandrup, J. and Immergut, E. H. (eds), *Polymer Handbook*, 3rd edn. Wiley, New York, 1989.
13. Wunderlich, B., *Macromolecular Physics*, Vol. 3. Academic Press, New York, 1980.
14. Martuscelli, E., Pracella, M. and Crispino, L., *Polymer*, 1983, **24**, 693.
15. Mezghani, K., Anderson, R. and Phillips, P. J., *Macromolecules*, 1994, **27**, 997.
16. Janimak, J. J., Cheng, S. Z. D., Zhang, A. and Hsieh, E. T., *Polymer*, 1992, **33**, 728.
17. Sanchez, I. C. and Eby, R. K., *Macromolecules*, 1975, **8**, 638.
18. Helfand, E. and Lauritzen, J. I., *Macromolecules*, 1973, **6**, 631.
19. Flory, P. J., *Trans. Faraday Soc.*, 1995, **51**, 848.
20. Cheng, S. Z. D., Janimak, J. J., Zhang, A., and Hsieh, E. T., *Polymer*, 1991, **32**, 648.
21. Avrami, M., *J. Chem. Phys.*, 1939, **7**, 1103; 1940, **8**, 212; 1941, **9**, 177.
22. Turner-Jones, A., *Polymer*, 1971, **12**, 487.
23. Glotin, M. and Mandelkern, L., *Colloid Polym. Sci.*, 1982, **260**, 182.
24. Alamo, R., Domszy, R. and Mandelkern, L., *J. Phys. Chem.*, 1984, **88**, 6587.
25. Ozawa, T., *Polymer*, 1971, **12**, 150.
26. Eder, M. and Wlochowicz, A., *Polymer*, 1983, **24**, 1593.